



W E S E

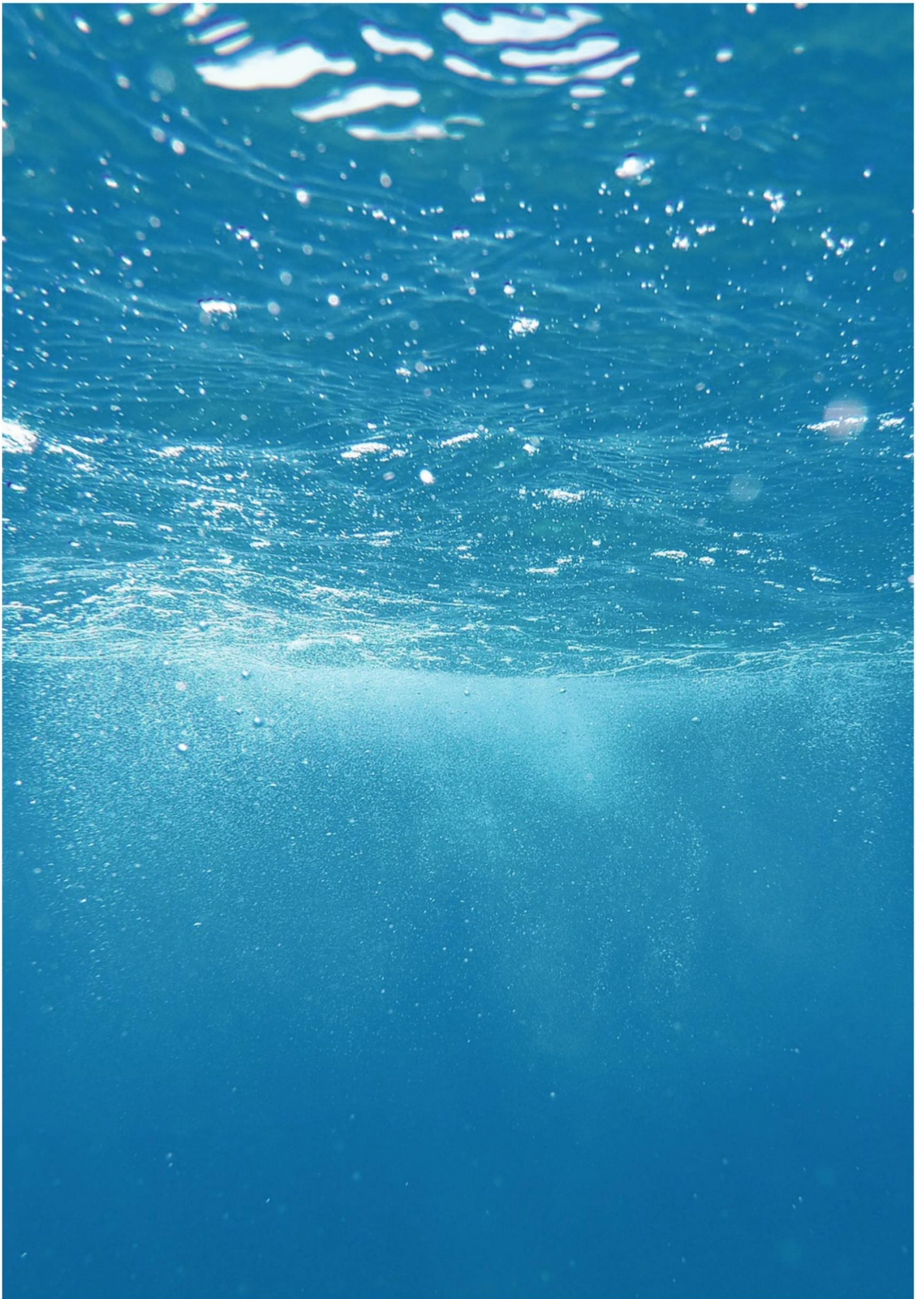
WAVE ENERGY
IN SOUTHERN EUROPE

DELIVERABLE 3.1 EMF Modelling



This project has been funded by the European Commission under the European Maritime and Fisheries Fund (EMFF), Call for Proposals EASME/EMFF/2017/1.2.1.1 – “Environmental monitoring of wave and tidal devices”. This communication reflects only the author’s view. EASME is not responsible for any use that may be made of the information it contains.





WP 3.1
Deliverable 3.1 EMF Modelling

PROJECT COORDINATOR
AZTI

TASK LEADER
WavEC

AUTHORS
Paulo Chainho – WavEC
Juan Bald - AZTI

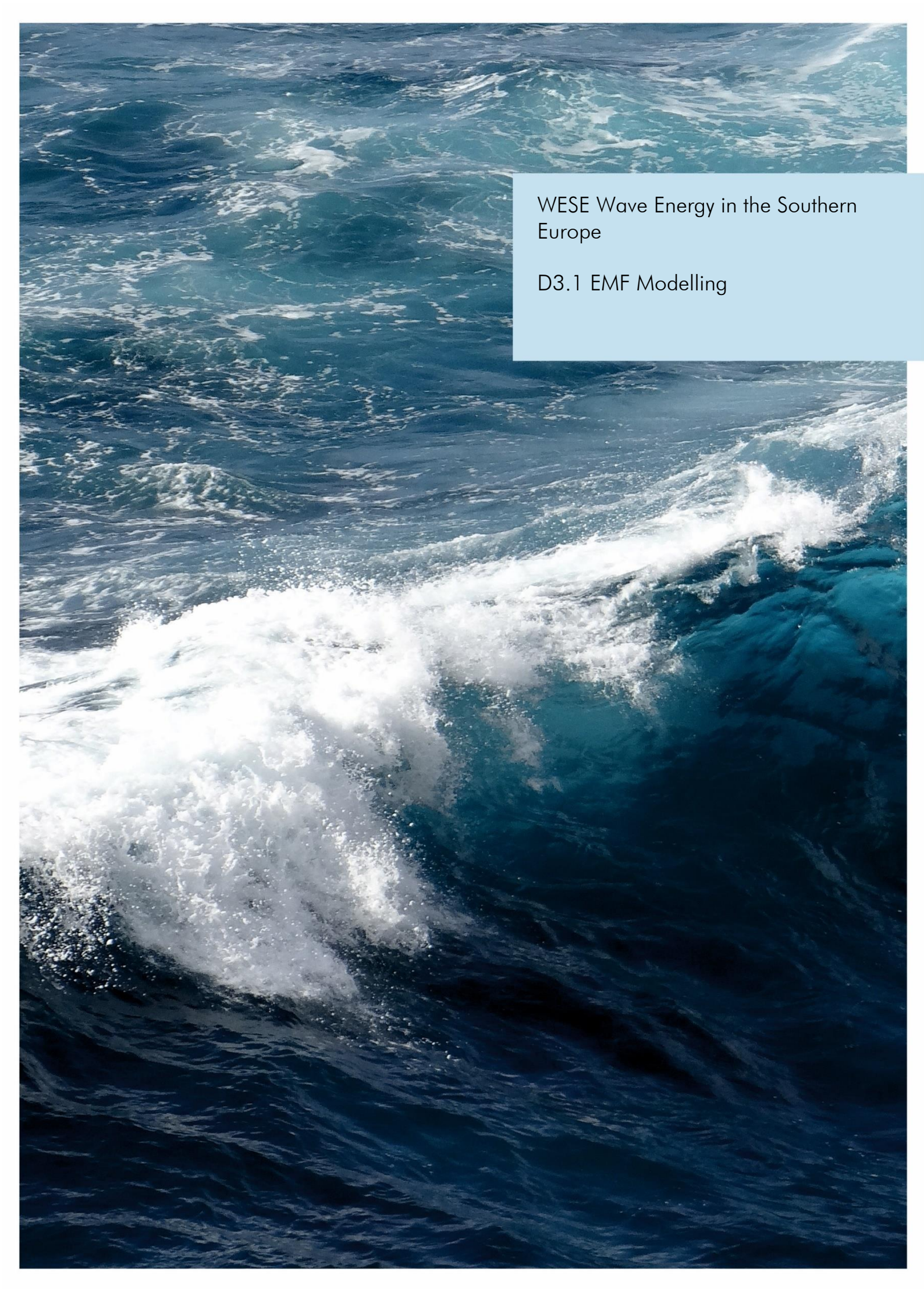
SUBMISSION DATE
04 | June | 2021

CITATION

Chainho P. and Bald J., 2021. Deliverable 3.1 (EMF Modelling). Corporate deliverable of the WESE Project funded by the European Commission. Agreement number EASME/EMFF/2017/1.2.1.1/02/SI2.787640. 30 pp.



This project has been funded by the European Commission under the European Maritime and Fisheries Fund (EMFF), Call for Proposals EASME/EMFF/2017/1.2.1.1 – “Environmental monitoring of wave and tidal devices”. This communication reflects only the author’s view. EASME is not responsible for any use that may be made of the information it contains.

An aerial photograph of the ocean showing a large, white, turbulent wake in the foreground, likely from a ship. The water is a deep blue color, and the wake is a bright white foam. The text is overlaid on a light blue rectangular background in the upper right quadrant.

WESE Wave Energy in the Southern
Europe

D3.1 EMF Modelling

CONTENTS

1. WESE PROJECT SYNOPSIS	6
2. EXECUTIVE SUMMARY	8
3. SUBMARINE POWER CABLES	9
3.1 BIMEP SUBMARINE POWER CABLE.....	10
3.2 PENICHE SUBMARINE POWER CABLE.....	12
4. EMF MODELLING	13
4.1 THEORY.....	13
4.1.1 <i>Magnetic Fields</i>	14
4.1.2 <i>Electric Fields</i>	16
4.2 FEMM MODEL.....	16
4.3 CASE STUDIES	19
4.3.1 <i>BIMEP – MARMOK-A-5</i>	19
4.3.2 <i>Peniche – Waveroller</i>	22
5. VALIDATION	26
6. CONCLUSIONS	28
7. REFERENCES.....	30



1. WESE project synopsis

The Atlantic seaboard offers a vast marine renewable energy (MRE) resource which is still far from being exploited. These resources include offshore wind, wave and tidal. This industrial activity holds considerable potential for enhancing the diversity of energy sources, reducing greenhouse gas emissions, and stimulating and diversifying the economies of coastal communities. Therefore, the ocean energy development is one of the main pillars of the EU Blue Growth strategy. While the technological development of devices is growing fast, their potential environmental effects are not well-known. In a new industry like MRE, and Wave Energy (WE) in particular, there may be interactions between devices and marine organisms or habitats that regulators or stakeholders perceive as risky. In many instances, this perception of risk is due to the high degree of uncertainty that results from a paucity of data collected in the ocean. However, the possibility of real risk to marine organisms or habitats cannot be ignored; the lack of data continues to confound our ability to differentiate between real and perceived risks. Due to the present and future demand for marine resources and space, human activities in the marine environment are expected to increase, which will produce higher pressures on marine ecosystems; as well as competition and conflicts among marine users. This context still continues to present challenges to permitting/consenting of commercial-scale development. Time-consuming procedures linked to uncertainty about project environmental impacts, the need to consult with numerous stakeholders and potential conflicts with other marine users appear to be the main obstacles to consenting WE projects. These are considered as non-technological barriers that could hinder the future development of WE in EU and Spain and Portugal in particular were, for instance, consenting approaches remain fragmented and sequential. Consequently, and in accordance with the Ocean Energy Strategic Roadmap published in November 2016¹, the main aim of the project consists on overcoming these non-technological barriers through the following specific objectives:

- Development of environmental monitoring around wave energy converters (WECs) operating at sea, to analyse, share and improve the knowledge of the positive and negative environmental pressures and impacts of these technologies and consequently a better knowledge of real risks.
- The resulting data collection will be used to apply and improve existing modelling tools and contribute to the overall understanding of potential cumulative pressures and impacts of larger scale, and future, wave energy deployments.

- Development of efficient guidance for planning and consenting procedures in Spain and Portugal for WE projects, to better inform decision-makers and managers on environmental real risks and reduce environmental consenting uncertainty of ocean WE introducing the Risk Based Approach suggested by the RiCORE, a Horizon 2020 project, which underline the difficulties for developers with an existing fragmented and sequential consenting approaches in these countries;
- Development and implementation of innovative maritime spatial planning (MSP) Decision Support Tools (DSTs) for Portugal and Spain for site selection of WE projects. The final objective of such tools will be the identification and selection of suitable areas for WE development, as well as to support decision makers and developers during the licensing process. These DSTs will consider previous findings (both environmental and legal, found in RiCORE) and the new knowledge acquired in WESE in order to support the development of the risk-based approach mentioned in iii);
- Development of a Data Sharing Platform that will serve data providers, developers and regulators. This includes the partners of the project. WESE Data Platform will be made of a number of ICT services in order to have: (i) a single web access point to relevant data (either produced within the project or by others); (ii) Generation of OGC compliant requests to access data via command line (advanced users); (iii) a dedicated cloud server to store frequently used data or data that may not fit in existing Data Portals; (iv) synchronized biological data and environmental parameters in order to feed models automatically.

2. Executive summary

The WP3 of the WESE project aimed to develop strategic research to address gaps in knowledge to improve modelling of potential cumulative pressures and environmental impacts of future WE deployments at larger scale. This deliverable reports the works of Task 3.1, aimed to investigate the EMF emitted by subsea power cables.

The main goal of Task 3.1 was to estimate the magnetic and electric field amplitude around the cables serving IDOM and Waveroller devices. The task description mentioned this goal would be achieved making use of commercial EMF modeling software, with the model estimates validated by comparison with the values measured in the field work, as described in EMF monitoring plans established under WP2.

The main goal was achieved, however by slightly different means. During the task development, the team concluded on the possibility of creating an open-source tool capable to estimate the EMF distribution around a three-phase cable design of adjustable dimensions, which would expand the added value to (and beyond of) the WESE project. Thus, while achieving the main goal, this task produced an open-source EMF modelling tool based on Python code and FEMM software. On the validation side, for a number of reasons described in (Paulo Chainho, 2020), it was not possible to gather quality EMF data, thus a comparison study was made with the outcomes of similar modeling studies, that proved high correlation.

3. Submarine Power Cables

Spanning over dozens of kilometers, subsea (or submarine) power cables are undoubtedly, the main source by footprint of EMF generated by offshore energy projects. This chapter presents the main characteristics of submarine power cables, which are relevant for understanding the EMF modeling work presented in this report.

Subsea power cables are composed of several layers. The overall design and materials do not differ much from cables installed ashore. Figure 1 illustrates the main components of a conventional three-phase HVAC submarine power cable.

Although the conductors can be made of alternatives like aluminium, the most frequently applied material is copper. These can either be composed of one single wire, stranded conductors, or profiled wire conductors, which provide a very smooth conductor surface.

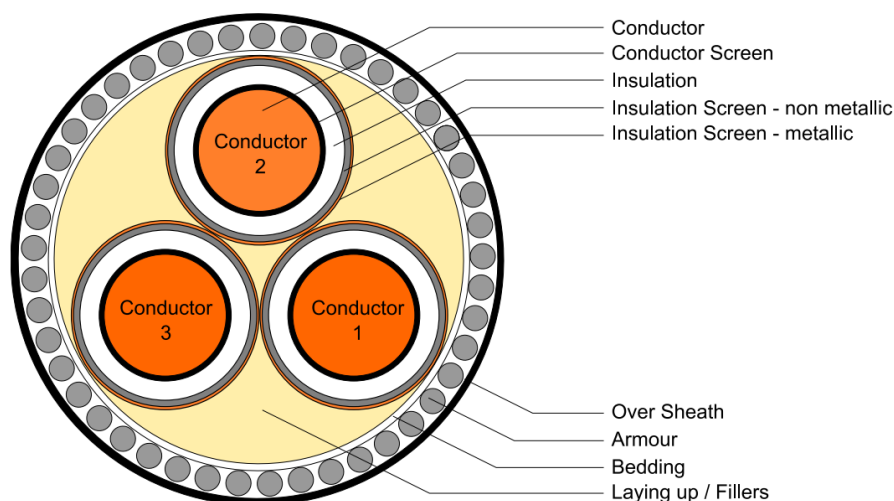


Figure 1. Typical 3-Phase Submarine Power Cable Sketch [IEC 605202-2].

Due to the applied electric potential, the conductors must be insulated by a proper dielectric material, with cross linked polyethylene (XLPE) being a common material used for the insulation. Beside its favorable dielectric properties, it is characterized by a comparatively high resistance to heat (operating temperature around 90°). Additionally, the insulation is coated with two 1-2mm thick layers (insulation and conductor screen). They guarantee a smooth surface, which results in decreased local stress enhancements, like notch effects. The screens thus improve the insulation durability by maintaining both mechanical properties and the related dielectric strength.

The laying up consists of fillers, which define the cylindrical cable shape and adds flexibility. It is enclosed by the bedding, which serves as an underlaying sheet for the armoring. The latter comprises a bundle of round wires with a diameter of two up to eight millimeters. The armour provides tension stability and mechanical protection during installation and operation (e.g. against fishing gear or anchors). It is the only element with physical properties and dimensions that affect significantly the internal and surrounding magnetic field. This property is referred to as magnetic permeability (μ), which defines the ability of a material to support the formation of a magnetic field within itself, thus, the higher the value the less resistant is the material to the passage of magnetic field lines. Table 1 shows the magnetic permeability and conductivity values of typical materials used in the construction of subsea cables. However, these should be accounted as average values only, since this property is typically nonlinear in ferromagnetic materials, and varies significantly with the magnetic field strength.

Table 1. Electromagnetic properties for cable components (CMASC, 2003).

	Permeability	Conductivity
Conductor	1.0	58.000.000
XLPE	1.0	0.0
Sheath (lead)	1.0	5.000.000
Armour (steel wire)	300	1.100.00
Seawater	1.0	5.0
Seabed	1.0	1.0

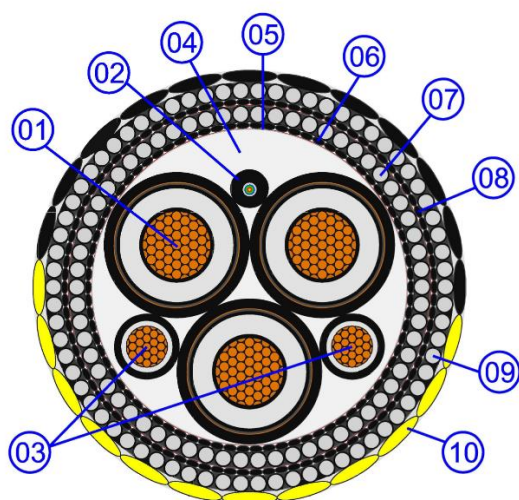
The armour can be made of ferrous (such as Electric Steel) or non-ferrous (such as copper) materials. Due to its relatively high magnetic permeability, ferrous materials concentrate the magnetic field around them, which reduces the magnetic field outside of the power cable.

3.1 BIMEP Submarine Power Cable

BIMEP test-site have 4 similar submarine power cables installed. These can be described as double armour, medium voltage power cables with an optical fiber unit, and 2 low voltage auxiliary power cables (Figure 2).

Relevant cable characteristics for the EMF studies are (Table 2): the overall cable dimensions, the armoring material and thickness, the conductor's distance (due to the canceling effect of the current lag between the three-phases), and any ferromagnetic metallic screens. This cable, as shown in Figure 2, has an overall diameter of 108 mm, is composed of a double armour of approximately 60 and 69 galvanized steel

wires, a three-phase 8.7/15kV export capacity composed of 3 stranded copper conductors with 185mm² cross section and XLPE insulation. For modeling simplicity, the 0.6/1kV auxiliary power cable will not be considered in this study.



No.	Description
01	3 off 185mm ² 8,7/15kV Power Cores A - 185mm ² Plain Copper Circular Stranded, Compacted and Waterblocked Conductor B - Extruded Semiconductive Conductor Screen C - XLPE Insulation (thickness: 4,5mm in accordance with IEC60502-2 table 6 and 7 for 8,7/15(17,5)kV Cables) D - Extruded Semiconductive Insulation Screen E - Semiconductive Waterswellable Tape F - Bare Copper Tapes Screen, hellically applied with overlap G - Extruded Polyethylene (LLDPE) Power Core Sheath
02	Fibre Optic Cable, 1x24 Opticals Fibres
03	Low Voltage Cables, 2x70mm ² 0,6/1kV
04	Polypropylene (PP) Yarns fillers
05	Binder Tape
06	Armour Bedding: Polypropylene (PP) fibrilated yarns
07	Armour (Layer 1): 4,0 mm Ø Galvanised Steel Wires (GSW) Armour with Bitumen Coating + Binder Tape
08	Separation Layer: Polypropylene (PP) fibrilated yarns
09	Armour (Layer 2): 4,0 mm Ø Galvanised Steel Wires (GSW) Armour with Bitumen Coating + Binder Tape
10	Outer Serving, Polypropylene yarns (PP)

Figure 2. BIMEP submarine power cable sketch.

Table 2. BIMEP Test-site cable specifications and components.

Subsea Cable General Specifications		
Rated Voltage	8.7/15 (17.5) kV	
Current carrying capacity	422 A	
Overall Diameter	108 mm	
Overall Weight (air)	25.5 kg/m	
Overall Weight (water)	18.5 kg/m	

Subsea Cable Components	Material	Dimensions
Conductor	Plain copper wires	Diameter – 15.9 mm
Conductor Screen	Extruded semi-conducting compound	Thickness – 1.0 mm
Insulation	XLPE compound	Thickness – 4.5 mm
Insulation Screen	Extruded semi-conducting compound	Thickness – 1.0 mm
Metallic Screen	1 layer with 2 bare copper tapes	Thickness – 0.1 mm
Inner Sheath	polyethylene LLDPE	Thickness – 2.2 mm
Bedding	polypropylene strings	Thickness – 2.0 mm
Wire Armour Layer 1	Galvanized steel wires	Diameter – 4.0 mm
Separation Layer	Polypropylene strings	Thickness – 2.0 mm
Wire Armour Layer 2	Galvanized steel wires	Diameter – 4.0 mm
Outer Sheath	Polypropylene strings	Thickness – 3.0 mm

3.2 Peniche Submarine Power Cable

The submarine power cable installed in Peniche test-site is a single armour, medium voltage power cable with an optical fiber unit, auxiliary power cable and a grounding conductor (Figure 3).

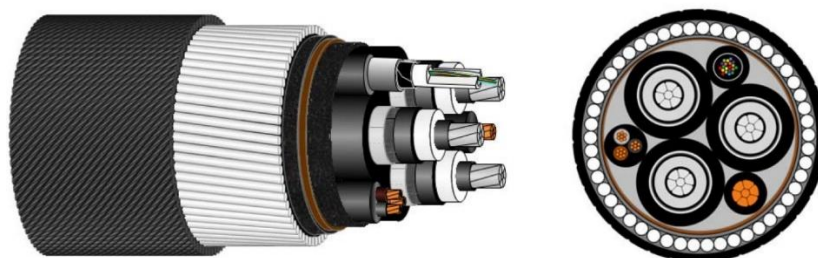


Figure 3. Peniche submarine power cable sketch.

Again, the relevant characteristics for the EMF studies are overall cable dimensions, the armoring material and thickness, the inter conductor's distance (due to the canceling effect of the current lag between the three-phases), and any ferromagnetic metallic screens. This cable, as shown in Table 3, has an overall diameter of 75mm, is composed of a single armour of approximately 45 galvanized steel wires, a three-phase 6/10kV export capacity composed of 3 stranded aluminum conductors with 50mm² cross section and XLPE insulation. For modeling simplicity, the 0.6/1kV auxiliary power cable will not be considered in this study.

Table 3. Peniche Test-site cable specifications and components.

Submarine Power Cable General Specifications		
Rated Voltage	6/10 (12) kV	
Current carrying capacity	125 A	
Overall Diameter	75 mm	
Overall Weight (air)	8.7 kg/m	
Overall Weight (water)	4.7 kg/m	
Subsea Cable Components	Material	Dimensions
Conductor	Round, stranded and compacted longitudinally watertight aluminium conductor	Diameter – 8.0 mm
Conductor Screen	Semi-conducting copolymer compound	Not Specified (assumed 0.2 mm)
Insulation	XLPE compound	Thickness – 3.4 mm
Insulation Screen	Semi-conducting copolymer compound, fully bonded to insulation	Thickness Not Specified (assumed 0.2 mm)
Metallic Screen	Longitudinal aluminum tape tightly bonded to sheath	Thickness – 0.2 mm
Inner Sheath	Black LLDPE compound	Thickness – 3.0 mm
Bedding	Semi-conducting water-swellaable tape	Thickness Not Specified (assumed 0.2 mm)
Wire Armour	Galvanized steel wires	Diameter – 4.0 mm
Outer Sheath	Bitumen, jute tape, layer of PP yarns	Thickness Not Specified (assumed 2.0 mm)

4. EMF Modelling

4.1 Theory

Energized subsea power cables are known sources of EM fields. As introduced in Deliverable 2.1 (Vinagre et al., 2019) [2], the electromagnetic field (EMF) can be described as a physically significant field generated by an electric charge. As the name suggests, EMF can be viewed as combination of two individual fields: the electric field (\vec{E}) and the magnetic field (\vec{B}), which are mutually dependent.

The magnetic fields can be generated by electric charges in motion (electric current), by varying electric fields and also by the intrinsic magnetic moments of a magnetic material (e.g. permanent magnets). While electric fields are of two kinds: Electrostatic field -> produced by stationary electric charges (e.g. electric potential difference – or voltage), and Induced electric field -> produced by time-varying magnetic fields. All these phenomena are present in energized subsea power cables.

With regards to the electrostatic field, these are confined between conductive elements with an electric potential difference. Since subsea cable conductors have a metallic shield covering the insulation which is generally grounded (zero potential), this guarantees the electric field is confined within the insulation. On the other hand, energized cables produce a magnetic field proportional to cable current. These magnetic field lines will be concentrated around materials with high magnetic permeability, thus, any ferromagnetic materials present in the cable, such as some types of the cable armoring, will have an attenuation effect with respect to the field intensity outside of the cable. Despite this attenuation effect, magnetic field lines are not fully contained within the cable.

Since the subsea power cables in this study have AC profiles, a time varying-magnetic field is expected outside of the cable, which induces electric fields as predicted by Maxwell Equations.

The Maxwell equations, considered among the most important equations in all of science, set the base for understanding the electromagnetic field theory. The chapters below presents a summary of the most relevant aspects to consider when attempting to model EM fields, for the particular case of submarine power cables.

4.1.1 Magnetic Fields

The baseline to quantify the magnetic field intensity outside of a power cable is described by the Ampere-Maxwell law. This law states “A circulating magnetic field is produced by an electric current and by an electric field that changes with time” (Fleisch, 2008). The corresponding equation quantifies the magnetic field by the sum of two terms, one proportional to the electric current, and another to the rate of change of an electric field. Minding that magnetic fields induced by changing electric fields are extremely weak (mostly relevant to problems at radio frequency levels -> from kHz to GHz), the later term can be neglected for the specific case of subsea power cables (Meeker, 2019) [4] which operate at 50Hz or 60Hz. Thus, for our problem the formula can be simplified, leaving only the terms associated with the Ampere law equation:

$$\oint_C \vec{B} \cdot d\vec{l} = \mu \cdot I_{enc} \quad (4.1)$$

Where, \oint_C is the line integral around the closed curve C , \vec{B} is the resultant vector of the magnetic field at the point of calculation (in Tesla units), $d\vec{l}$ is an infinitesimal element of the curve C (in meters), μ is the magnetic permeability of the medium (where in vacuum $\mu = \mu_r \mu_0 = 1 \times 4\pi \times 10^{-7} H \cdot m^{-1}$) and I_{enc} the current flowing through the closed curve C (in ampere units).

For better understanding how this formula applies to a subsea power cable, let's assume an infinite long and straight conductor. When this conductor carries carrying a current I , the resulting magnetic field lines are concentric circles surrounding the conductor center, as shown in the Figure 4.

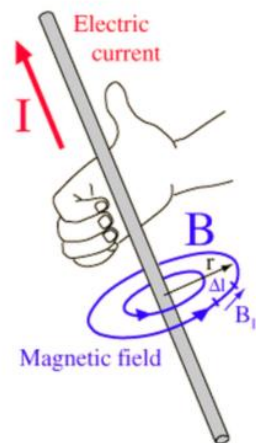


Figure 4. Magnetic field lines surrounding a straight long conductor, as per the *Right hand rule* mnemonic.

The amplitude of \vec{B} is the same in every point of the concentric circle with radial distance r , meaning the line integral from Eq. (4.1) is equal to the sum of the magnetic field vector along the concentric circle, which returns $\oint_c \vec{B} \cdot d\vec{l} = B(2\pi r)$. The magnetic field for this problem can then be computed with the following:

$$\vec{B} = \frac{\mu I}{2\pi r} \hat{\phi} \quad (4.2)$$

With the direction being unit vectors $\hat{\phi}$ tangential to the concentric circle, shown in Figure 4 as per the right-hand rule.

The problem described in the previous paragraphs assumes a single long and straight conductor, however, as presented in section 3, submarine power cables are usually part of a three-phase power system, with the three conductors placed symmetrically inside the subsea cable. In this case, these three conductors carry a three-phase current which individually generate magnetic field lines with the same properties as described in Eq. (4.2). These fields are added together to the resulting magnetic field, which is the sum of the individual vector fields generated from the cable conductors. As described by Eq. (4.2), the contribution of each individual conductor to the magnetic field is dependent on the distance of each conductor to the point of measurement, and the amplitude of the current at the time of measurement. Three-phase currents have a phase shift of one-third cycle (120° or $2\pi/3$ radians), in time domain this returns.

Assuming an arbitrary point of measurement P, the magnetic field as per Eq. (4.2), can be computed from the instant current amplitude at each of the 3 conductors, and the distance from the conductors. Mathematically this complex interaction can be described as a superposition of three single fields surrounding their respective conductors. Figure 5 provides a visual representation.

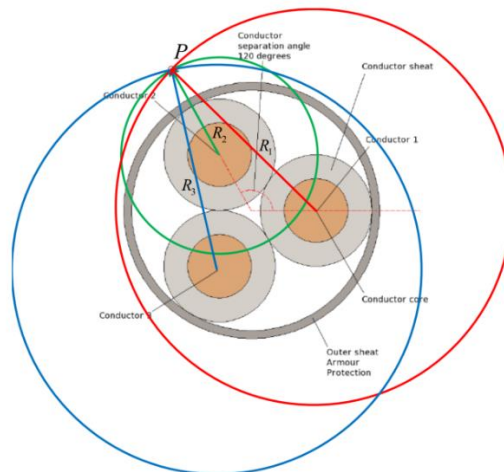


Figure 5. Three-phase cable cross section, with P being the point of measurement, and R1 R2 and R3 the distance from the conductors to the point of measurement.

4.1.2 Electric Fields

There are two different sources of electric fields, one created by stationary electric charges, referred to as electrostatic field and one created by a changing magnetic field, referred to as induced electric field. Both are vector units with a direction and magnitude, measured in $V \cdot m^{-1}$, with the net value at any point being the vector sum of all the electric fields present at that point.

An electrostatic field is present in all live power cables, as the system voltage results in an electric potential difference between the conductors and the remaining environment. Nowadays, it is a common practice to ground the conductor metallic sheathes (for safety and reliability purposes) which guarantees this component has a zero-electric potential. This confines the electrostatic field within the individual conductors, as this E-field will be radially distributed inside the dielectric insulation from the conductor core to the metallic sheathes. Therefore, this E-field source is not expected outside of the cable if proper cable earthing is achieved (CMASC, 2003). Thus, for AC subsea power cables, only electric field produced by the varying magnetic field is emitted into the marine environment. The Faraday law of induction sets the base to understand this principle.

$$\oint_C \vec{E} \cdot d\vec{l} = -\frac{d}{dt} \int_S \vec{B} \cdot \hat{n} da \quad (4.2)$$

This law states “A circulating electric field is produced by a magnetic field that changes with time” (Fleisch, 2008). Also relevant to our case, is to mention that an electric field applied to a conductive medium (e.g. seawater) will cause electric currents to flow in that material, hence, the electric current density is directly proportional to the electrical field: $\vec{j} = \sigma \vec{E}$, with the constant of proportionality being the medium conductivity.

4.2 FEMM Model

The differential equations shown in the previous section appear to be relatively compact, however, the complexity of combining a three-phase system and cable geometries with different materials (e.g. steel and copper) within different mediums (e.g. seabed and seawater), suggested that a finite element method should be used to model this problem.

Several software packages are available to model magnetic and electric fields. Based on the team previous experience with different tools, the software package - Finite Element Method Magnetics (FEMM) (Meeker, 2019) - was viewed as the most suitable

option for the WESE project characteristics. FEMM is a simple, low computational cost software package for solving electromagnetic projects using finite element method, its features are proven and have been used extensively in academic studies (Petkovska, L. and G. Cvetkovski, 2005; Sinnadurai, 2007; Mohanraj et al., 2021), covering the needs for modeling the EMF generated by submarine power cables. A list of its most relevant features and reasoning for the WESE project are compiled below:

- FEMM is an open-source software, which allows for all the code and outcomes of this task to be accessible and can be replicated by anyone interested in the topic with little coding skills. This is particularly relevant as the commercial software's available for modelling EMF's can cost more than 10k€'s per license.
- FEMM has an API framework with the open-source programming language – Python – which was used to develop an automated code routine capable of generating specific submarine cable designs, based on few dimension inputs.
- FEMM solver addresses low frequency electromagnetic problems in two-dimensional planar domains. This perfectly captures the problem of studying EMFs generated by submarine power cables, as the grid frequency where the cables operate is typically 50Hz or 60Hz, fitting well into the time-harmonic domain of the solver. Plus, since each cable cross-section is unique, the 2D planar design is valid at any point along its cable length.

As mentioned, the open-source modelling tool is based on Python code and pyFEMM, a Python package that allows to operate the Finite Element Method Magnetics (FEMM) software via a library of Python functions. Figure 6 presents a flowchart of the algorithm main inputs and processes.

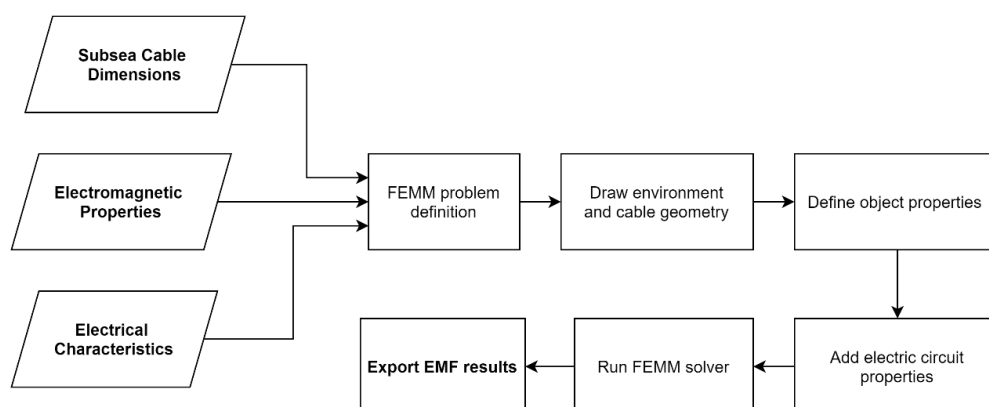


Figure 6. EMF modelling tool flowchart.

As expected, the algorithm follows closely FEMM’s processing routines, adapted specifically for the design and analysis of subsea power cables. More detail about each block is presented in the table below.

Table 4. Flowchart blocks of FEMM model (input and processes).

Flowchart blocks		Description
Inputs	Subsea Cable Dimensions	<ul style="list-style-type: none"> • Conductor cross sectional area (mm²) • Conductor screen thickness (mm) • Conductor insulation thickness (mm) • Conductor insulation nonmetallic screen thickness • Conductor insulation metallic screen thickness (mm) • Bedding thickness (mm) • Armour radius (mm) • 2nd Armour layer radius (mm) -> set 0 if non-existent • Over Sheath thickness (mm) • Burial depth [mm] -> set 0 if surface laid
	Electromagnetic properties	Definition of the conductivity (S/m) and relative permeability (unitless) of all objects: <ul style="list-style-type: none"> • Conductors • Insulation • Nonmetallic Insulation Screen • Metallic Insulation screen • Inner Sheath • Bedding • Armour • Over sheath • Seawater • Seabed
	Electrical Characteristics	<ul style="list-style-type: none"> • RMS Phase Current (A) • Grid frequency (Hz)
Processes	FEMM problem definition	This block initializes a FEMM process and specifies the overall definitions: problem type (magnetics), problem frequency (Hz), units (millimeter), AC solver (successive approximation), solver precision (10 ⁻⁸), type (planar), depth (5000mm) and mesh min. angle (30°)
	Draw environment and cable geometry	Using the subsea cable dimensions, a set of geometric and trigonometric principles is used to sequentially draw all cable elements, using lines and arc’s segments as defined by pyFEMM functions.
	Define object properties	With the cable contour circles drawn, the material electromagnetic properties inputs are used to define the specific characteristics of each enclosed contour.
	Add electric circuit properties	To define the current flowing inside each conductor, FEMM uses circuit blocks. Minding the system is oscillating at one fixed frequency, the 3-phase current “phasors” can be represented by complex numbers: $I_1 = \text{AMPS} + 0j$ $I_2 = -0.5 * \text{AMPS} + \text{AMPS} * 0.866j$ $I_3 = -0.5 * \text{AMPS} - \text{AMPS} * 0.866j$ Where AMPS is the peak phase current, computed from the RMS input value.
	Run FEMM solver	With the problem fully defined (cable geometry, cable and environment properties and circuit properties), the algorithm calls the FEMM solver, which runs the mesh generator and executes the time-harmonic problem solver.
Export EMF results	After successfully running the solver, outputs are extracted and post-processed, specifically: <ul style="list-style-type: none"> - The absolute value of the magnetic flux density (B) - The absolute value of the current density (J), which is converted to electric field using the $\vec{J} = \sigma \vec{E}$ equation. Horizontal and radial line plots are exported both in graphical form and to .csv files.	

The open-source code of the EMF modelling tool can be found in WavEC’s public repository, through the following link:

https://github.com/WavEC-Offshore-Renewables/EMF_modeling_tool

It requires Python 3.7 version, plus the installation of pyFEMM package.

4.3 Case studies

WESE project scope includes three main wave energy projects, from which two have submarine power cables as part of the infrastructure, namely: MARMOK-A-5 device installed in BIMPEP test site in Spain, and Waveroller device installed off the coast of Peniche in Portugal. As defined in D2.1 report of this project (Vinagre et al., 2019), these two projects have in-situ EMF monitoring plans, and thus should be modelled with the acquired monitoring results allowing for model validation. However, as presented in D2.2 report (Chainho, P. and Bald, J., 2020), for a number of reasons in neither of the sites it was possible to gather quality EMF data, thus, to validate the modelling results, this report will rely on previous research conducted in the same field, namely the Electromagnetic Field Study funded by Oregon Wave Energy Trust (Slater et al., 2010).

Making use of the generic EMF modelling tool for submarine power cables described in the previous section, the two case studies here presented model the specific submarine cable design and associated project electrical characteristics.

4.3.1 BIMPEP – MARMOK-A-5

As depicted in section 3.1, BIMPEP test site have 4 similar subsea power cables, one of which have recently hosted the first floating wave energy device connected to the grid in Spain, the MARMOK-A-5 device. This case study will model BIMPEP specific cable design, and will make use of the cable voltage and device power to compute the maximum cable current to be used, considering the following equation $P = \sqrt{3} \cdot V_{LL} \cdot I \cdot \text{pf}$, where P is the power capacity of each device, V_{LL} is the line to line voltage of the 3-phase transmission system, I is the phase current (variable of interest) and pf is the power factor.

Table 5 shows the computed phase current for the MARMOK-A-5 device installed in BIMPEP, producing at rated power and assuming the power factor is equal to one.

Table 5. BIMPEP – MARMOK-A-5 Maximum cable current.

	Device Power (P)	Transmission Voltage (VLL)	Phase Current (I)
BIMPEP – MARMOK-A-5	30 kW	13.2 kV	1.3 A

With this data, the modeling process follows the methodology described in section 4.2. Using the cable design as specified in **Error! No se encuentra el origen de la referencia.**, the cable model was created from the component dimensions and corresponding materials. Then, after specifying the cable current and defining proper mesh size, the FEMM solver was used to compute the EMF radiated. Figure 7 shows a graphic representation of this sequence.

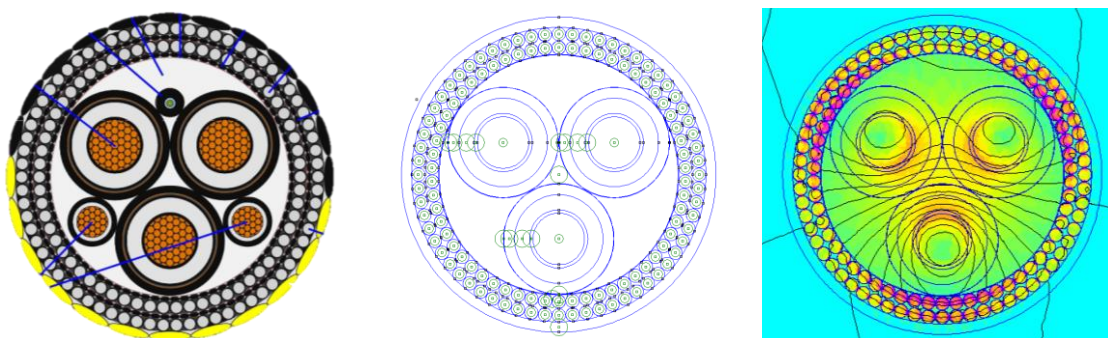


Figure 7. BIMEP cable drawing (left), BIMEP cable model generated in FEMM (center) and Finite element analysis of the EMF's (right).

The first subset of results is shown in Figure 8, these correspond to the scenario where the BIMEP cable is surface laid on the seabed. As expected, the magnetic flux density $|B|$ maximum value is observed close to the cable surface, measuring $0.40\mu\text{T}$. These show a close to exponential decay with distance, with magnetic field reduced to $0.008\mu\text{T}$ when distanced 1 meter away from the cable. The electric field show a similar pattern as are essentially induced by the same varying magnetic field. Close to the cable surface, the electric field has a value of $13\mu\text{V}\cdot\text{m}^{-1}$, decaying to $2\mu\text{V}\cdot\text{m}^{-1}$ when distanced 1 meter away from the cable.

As shown in section 4.1, the magnetic and electric induced fields are linearly proportional to the electric current, hence another way to present the EMF modeling results, is per current unit (ampere), which allows to extrapolate to other current levels, these results are shown in Figure 9. Since the voltage level of the cables is known, in BIMEP case $V_{LL} = 13.2\text{kV}$, the equation $P = \sqrt{3} \cdot V_{LL} \cdot I \cdot \text{pf}$ allows to present the curves per power unit (kilowatt), these are shown in Figure 10.

As an exercise, with these curves one can estimate the maximum EMF levels emitted by this cable if ever operated at its maximum current carrying capacity (of 422A as shown in Table 2). For such current amplitude, the EMF levels would be $127\mu\text{T}$ and $4.2\text{mV}\cdot\text{m}^{-1}$ near the cable surface, and $2.74\mu\text{T}$ and $675\mu\text{V}\cdot\text{m}^{-1}$ when distanced 1 meter away from the cable.

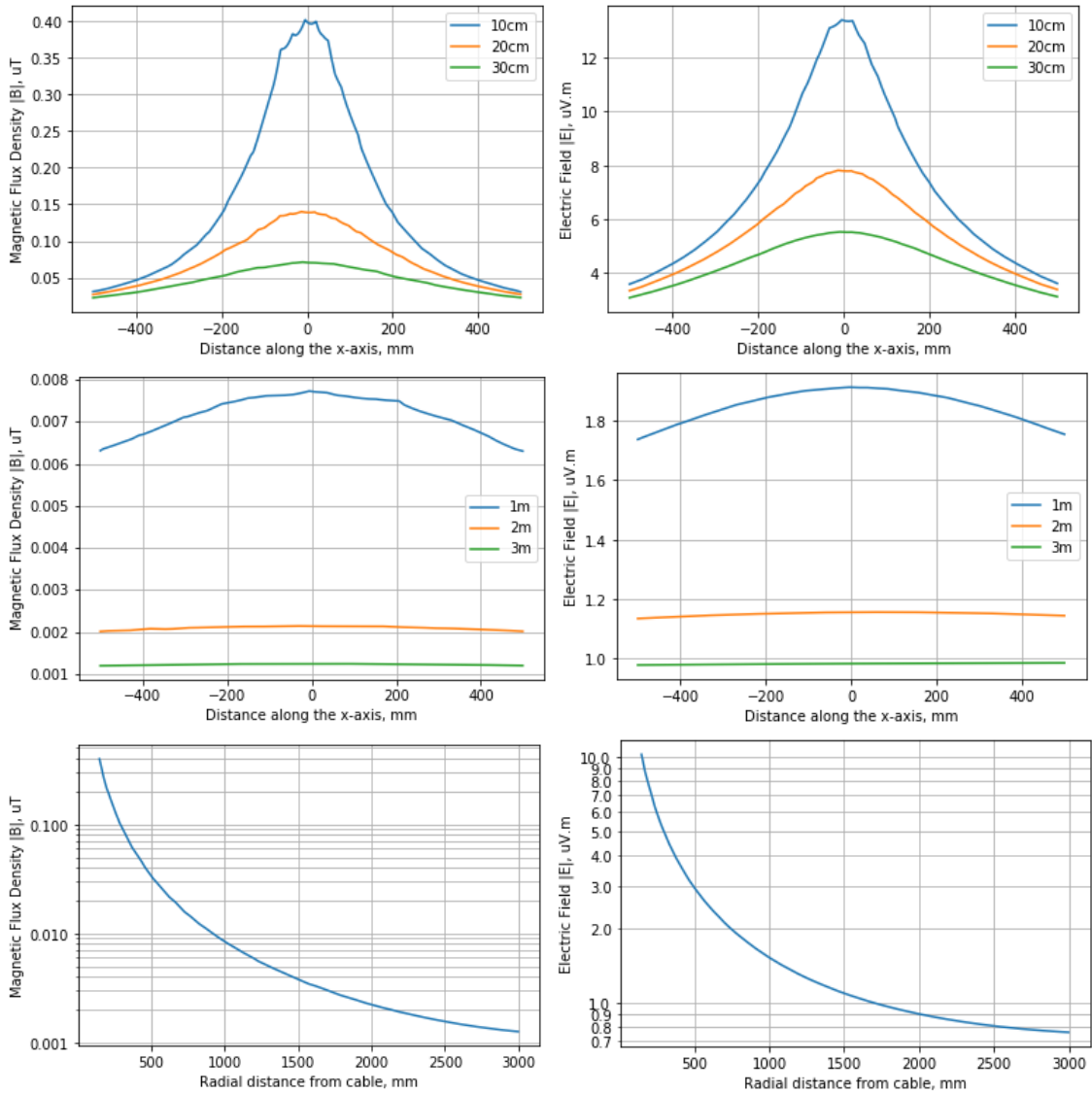


Figure 8. EMF modelling results from BIMEP cable at device rated power (top) at a distance of 10/20/30cm parallel to the cable surface (middle) at a distance of 1/2/3m parallel to the cable surface (bottom) Radial distance from the cable surface.

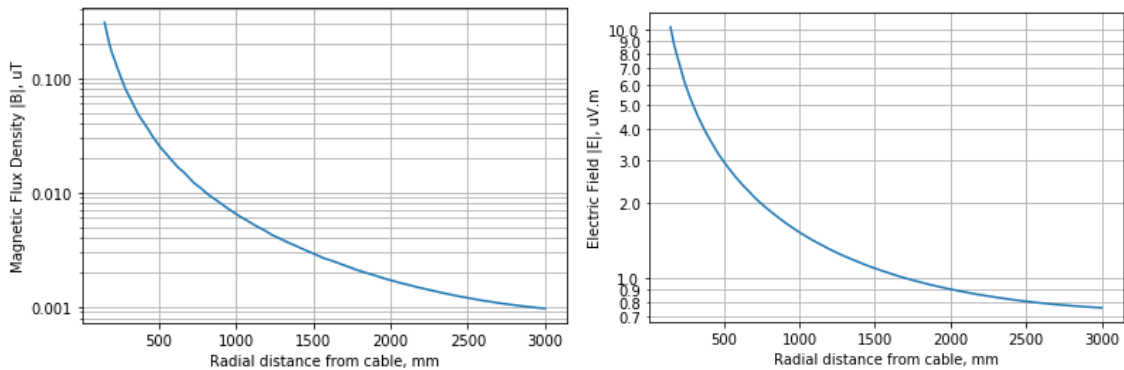


Figure 9. EMF modelling results from BIMEP cable per ampere.

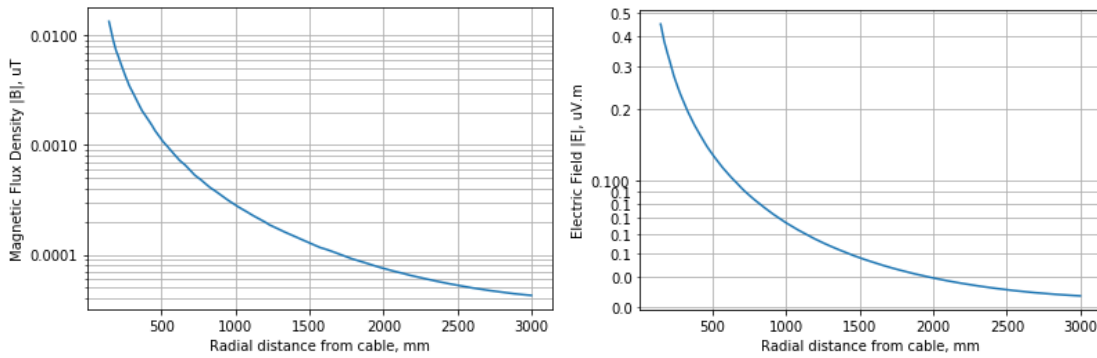


Figure 10. EMF modelling results from BIMEP cable per kW.

4.3.2 Peniche – Waveroller

As depicted in section 3.2, Peniche test site have one medium voltage submarine power cable, serving a single seabed mounted wave energy device, called the Waveroller. This case study will model Peniche cable design, and will make use of the cable voltage and device power to compute the maximum cable current to be used, considering the following equation $P = \sqrt{3} \cdot V_{LL} \cdot I \cdot \text{pf}$, where P is the power capacity of each device, V_{LL} is the line to line voltage of the 3-phase transmission system, I is the phase current (variable of interest) and pf is the power factor.

Table 6 shows the computed phase current for the Waveroller device installed in Peniche, producing at rated power and assuming the power factor is equal to one.

Table 6. Peniche – Waveroller Maximum cable current.

	Device Power (P)	Transmission Voltage (VLL)	Phase Current (I)
Peniche - Waveroller	420 kW	10 kV	24.2 A

With this data, the modeling process follows the methodology described in section 4.2 -> using the cable design as specified in Table 3, the cable model was created from the component dimensions and corresponding materials. Then, after specifying the cable current and defining proper mesh size, the FEMM solver was used to compute the EMF radiated. Figure 11 shows a graphic representation of this sequence.

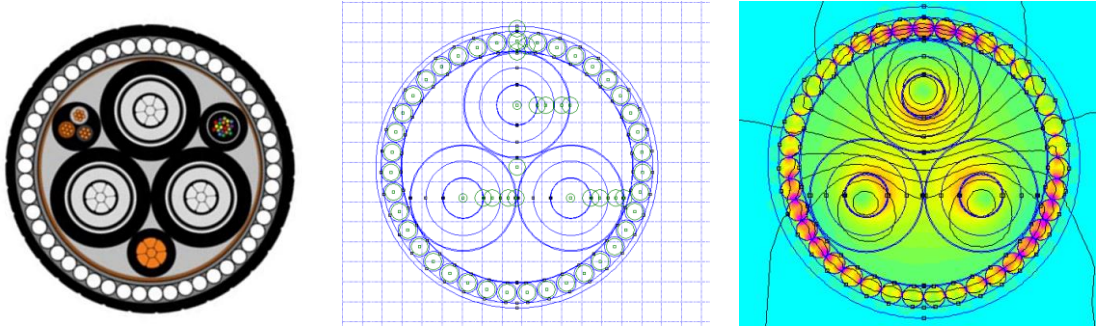


Figure 11. Peniche cable drawing (left), Peniche cable model generated in FEMM (center) and Finite element analysis of the EMF's (right).

The results are shown in Figure 12, these correspond to the scenario where Peniche power cable is surface laid on the seabed. As expected, the magnetic flux density $|B|$ maximum value is observed close to the cable surface, with an amplitude of $7\mu\text{T}$. The magnetic field show a close to exponential decay with distance, with amplitude reduced to $0.11\mu\text{T}$ when distanced 1 meter away from the cable. The electric field show a similar pattern as are essentially induced by the same varying magnetic field. Close to the cable surface, the electric field shows a value of $215\mu\text{V}\cdot\text{m}^{-1}$, decaying to $29\mu\text{V}\cdot\text{m}^{-1}$ when distanced 1 meter away from the cable.

As shown in section 4.1, the magnetic field is linearly proportional to the electric current, hence another way to present the EMF modeling results, is per current unit (ampere), which allows to extrapolate to other current levels, these results are shown in Figure 13. Since the voltage level of the cables is known, in BIMEP case $V_{LL} = 10\text{kV}$, the equation $P = \sqrt{3} \cdot V_{LL} \cdot I \cdot \text{pf}$ allows to present the curves per power unit (kilowatt), these are shown in Figure 14.

As an exercise, one can estimate the maximum EMF levels emitted by this cable if ever operated at its maximum current carrying capacity (of 125A as shown in Table 3). For such current amplitude, the magnetic and electric field amplitudes close to the cable surface, would be of $37.5\mu\text{T}$ and $1.1\text{mV}\cdot\text{m}^{-1}$ respectively, and $0.63\mu\text{T}$ and $150\mu\text{V}\cdot\text{m}^{-1}$ when distanced 1 meter away from the cable.

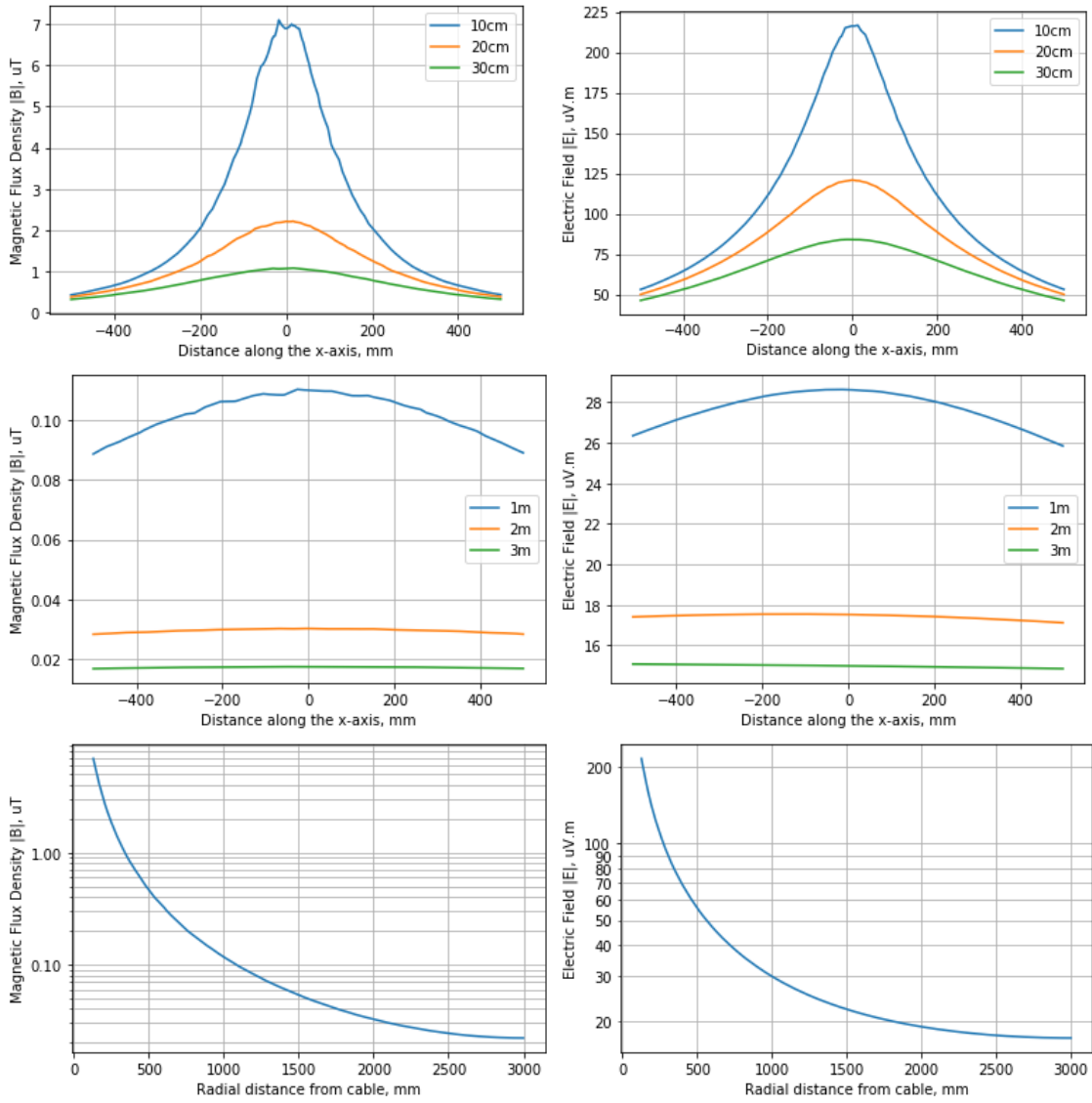


Figure 12. EMF modelling results from Peniche submarine power cable at device rated power (top) at a distance of 10/20/30cm parallel to the cable surface (middle) at a distance of 1/2/3m parallel to the cable surface (bottom) Radial distance from the cable surface rated power.

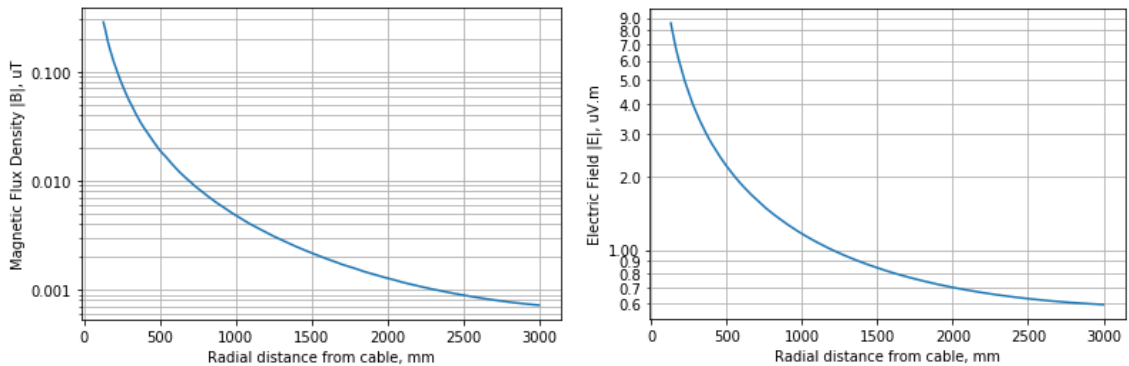


Figure 13. EMF modelling results from Peniche cable per ampere.

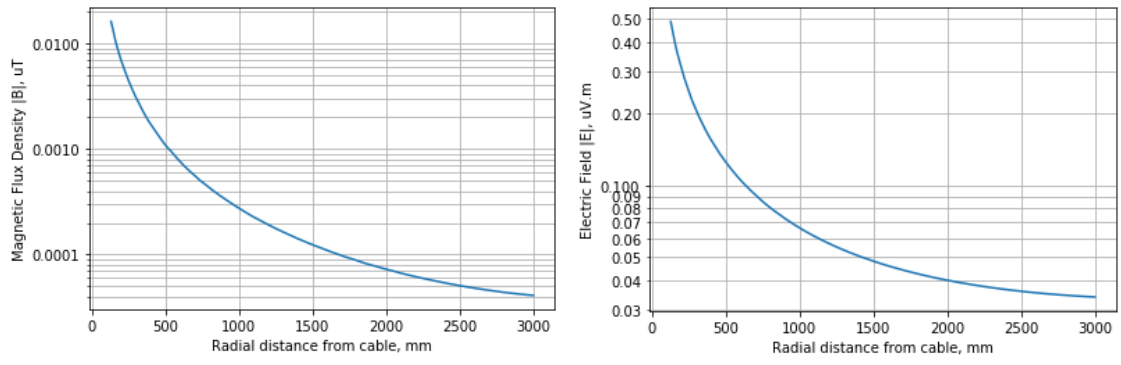


Figure 14. EMF modelling results from Peniche cable per kW.

5. Validation

As previously mentioned, the two WEC projects presented in the previous section had EMF monitoring campaigns plans in place, that would be used to support the modelling approach and results. For a number of reasons (specified in D2.2 of this project (Chainho, P. and Bald, J., 2020)), in neither of the sites was possible to gather quality EMF data. Thus, to validate the modelling results, this report will rely on previous research conducted in the same field, namely the Electromagnetic Field Study funded by Oregon Wave Energy Trust (OWET) (Slater et al., 2010). This study also investigates the electromagnetic fields generated by WEC projects and looks specifically to subsea power cables. Within the project results, one report provides log-log scale plots, of normalized (per current unit) values of Electric and Magnetic fields generated by a generic 3-phase power cable with single armour (cable component dimensions are not clear in the report), shown in Figure 15. Similar normalized plots were compiled for Peniche and BIMEP case studies, as shown in Figure 9 and Figure 13 included in the previous section.

Worth mentioning that the OWET results are based on a Finite Element Analysis (FEA) using Ansoft Maxwell 2D™, thus a comparison exercise can only corroborate our numerical modelling approach, but not the actual values, as these are not validated against experimental data.

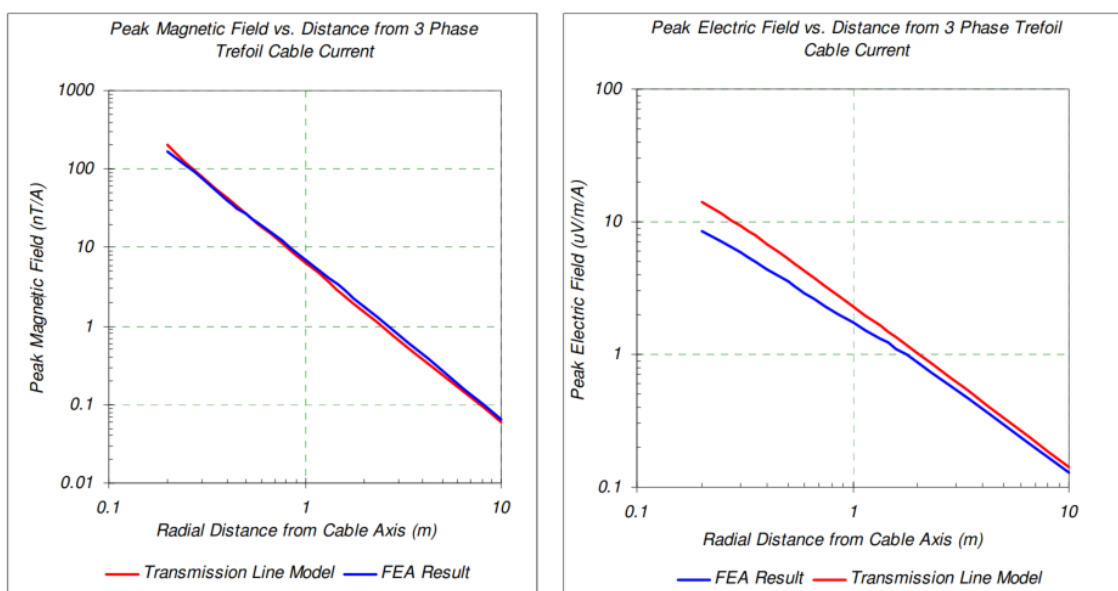


Figure 15. Normalized Electric and Magnetic fields generated by a 3-phase power cable as shown in (Slater et al., 2010).

As discussed in section 4.1, the magnetic and electric induced fields are linearly proportional to the electric current, using normalized per current unit results removes the current/power levels from the comparison. Although the cable structure is similar (3-phase power cable with single armour), the actual cable dimensions were not clear in the OWET report and cannot be compared to the ones used our two case studies.

Table 7 presents a comparison table, with the OWET results retrieved from approximate visual interpretation of the Figure 15, next to the numerical result outputs from our two case studies. Despite the possible differences in cable dimensions, the results from both case studies show close correlation with the OWET study. With deviations from 7% to 56%, the larger differences occur near the cable surface, as expected due to differences in cable dimensions.

Table 7. Comparison between normalized (per current unit) values of Electric and Magnetic fields from the Oregon study and the open-source EMF modelling tool.

Radial Distance	OWET Study – FEA Result		BIMEP – IDOM		PENICHE – Waveroller	
	Magnetic Field	Electric Field	Magnetic Field	Electric Field	Magnetic Field	Electric Field
0.2 m	200 nT	9 μV/m	300 nT	10 μ V/m	300 nT	9 μ V/m
0.5 m	11 nT	3 μV/m	25 nT	3 μ V/m	19 nT	2.2 μ V/m
1.0 m	7 nT	1.7 μV/m	6.5 nT	1.6 μ V/m	5 nT	1.3 μ V/m
2.0 m	2 nT	0.8 μV/m	1.8 nT	0.9 μ V/m	1.4 nT	0.7 μ V/m
3.0 m	0.7 nT	0.5 μV/m	1 nT	0.8 μ V/m	0.7 nT	0.6 μ V/m

6. Conclusions

The main goal of Task 3.1 was to estimate the magnetic and electric field amplitude around the cables serving IDOM and Waveroller devices. The task description mentioned this goal would be achieved making use of commercial EMF modeling software, with the model estimates validated by comparison with the values measured in the field work, as described in EMF monitoring plans established under WP2.

The main goal was achieved, however by slightly different means. During the task development, the team concluded on the possibility of creating an open-source tool capable to estimate the EMF distribution around a three-phase cable design of adjustable dimensions, which would expand the added value to (and beyond of) the WESE project. Thus, while achieving the main goal, this task produced an open-source EMF modelling tool based on Python code and FEMM software.

In Section 3, the report starts by presenting the main characteristics of submarine power cables, the main source by footprint of EMF generated by ocean energy projects, with particular focus on the two-project specific subsea cables to be evaluated within this task (BIMEP and Peniche test-sites). This is followed by Section 4, which begins with a short overview of the theory around EMF, supporting the choice of finite element method approach for the modelling exercise. Next, the EMF model is described, with particular attention to the open-source reasoning, and in particular for choosing FEMM software.

Section 4.3 describes in detail the two-case studies originally included in this task, followed by the corresponding EMF modelling results. In general, both case studies show small EMF impact. The BIMEP subsea cable serving IDOM device (operating at rated power) show amplitudes of $|B| = 0.40\mu\text{T}$ and $|E| = 13\ \mu\text{V}\cdot\text{m}^{-1}$ close to cable surface, with rapid decay to $|B| = 0.008\mu\text{T}$ and $|E| = 2\ \mu\text{V}\cdot\text{m}^{-1}$ when distanced 1 meter away from the cable. The Peniche subsea cable serving the Waveroller device (also operating at rated power) show amplitudes of $|B| = 7\mu\text{T}$ and $|E| = 215\ \mu\text{V}\cdot\text{m}^{-1}$ close to cable surface, with rapid decay to $|B| = 0.11\mu\text{T}$ and $|E| = 29\ \mu\text{V}\cdot\text{m}^{-1}$.

The rather small EMF impact can be attributed to the small cable currents, or in other words, to the cables being oversized for the power capacity of the devices. Thus, in order to access the impact of increasing the number of devices, the EMFs were also estimated for the maximum current capacity of both power cables. The BIMEP subsea cable operating at its maximum current of 422A (corresponding to 9.6MVA), would see the EMF levels raise to $|B| = 127\mu\text{T}$ and $4.2\text{mV}\cdot\text{m}^{-1}$ near the cable surface, and

$|B| = 2.74\mu\text{T}$ and $675\mu\text{V.m}^{-1}$ when distanced 1 meter away from the cable. For the Peniche subsea cable operating at its maximum current of 125A (corresponding to 2.2MVA), the EMF levels would raise to $|B| = 37.5\mu\text{T}$ and $|E| = 1.1\text{mV.m}^{-1}$ respectively, and $|B| = 0.63\mu\text{T}$ and $|E| = 150\mu\text{V.m}^{-1}$ when distanced 1 meter away from the cable.

Overall, this report provides access to an open-source modelling tool, capable to compute the EMF generated by any three-phase cable design. With this tool, the report presents the computed results for two case studies. The EMF shows an exponential decay with distance, with the computed amplitudes being reduced by at least one order of magnitude when distanced 1 meter from the cable source. Minding the EMF amplitude being linearly proportional to the electric current, the results can be extrapolated for any cable current. Finally, without in-situ measurements available, the model outputs are compared to the results of similar modeling studies, that proved high correlation.

7. References

Chainho P., Bald J., 2020. Deliverable 2.2 (Monitoring of Electromagnetic fields). Corporate deliverable of the WESE Project funded by the European Commission. Agreement number EASME/EMFF/2017/1.2.1.1/02/SI2.787640. 55 pp

CMACS (2003). A baseline assessment of electromagnetic fields generated by offshore windfarm cables. Birkenhead (UK), Centre for Marine and Coastal Studies, University of Liverpool: 71.

Fleisch, D., 2008. A Student's Guide to Maxwell's Equations, Cambridge University Press, New York (USA). 134 pp.

Meeker, D.C., " Finite Element Method Magnetics, Version 4.2 (21April 2019 Build)," [Online - <https://www.femm.info/wiki/HomePage>].

Mohanraj, G. T., M. R. Rahman, S. Joladarashi, H. Hanumanthappa, B. K. Shanmugam, H. Vardhan and S. A. Rabbani, 2021. Design and fabrication of optimized magnetic roller for permanent roll magnetic separator (PRMS): Finite element method magnetics (FEMM) approach. Advanced Powder Technology, 32 (2):546-564.

Petkovska, L. and G. Cvetkovski, 2005. Steady State Performance Evaluation of a Permanent Magnet Synchronous Motor Based on FEA.

Sinnadurai, R., 2007. Modeling of a Three Phase Linear Generator by Using Finite Element Magnetics Method. Proceedings of ENCON2007, 1st Engineering Conference on Energy & Environment. December 27-28, 2007, Kuching, Sarawak, Malaysia. 2005-2010 pp.

Slater, M., Jones, R., Schultz, A., 2010. Electromagnetic Field Study - The prediction of electromagnetic fields generated by submarine power cables. Oregon WaveEnergy Trust. 47 pp.

Vinagre P.A., Cruz E., Chainho P., Ruiz P., Felis I., Muxika I., Bald J., 2019. Deliverable 2.1 Monitoring plans for Noise, Electromagnetic Fields and Seabed Integrity. Corporate deliverable of the Wave Energy in the Southern Europe (WESE) Project funded by the European Commission. Agreement number EASME/EMFF/2017/1.2.1.1/02/SI2.787640. 60 pp.



This project has been funded by the European Commission under the European Maritime and Fisheries Fund (EMFF), Call for Proposals EASME/EMFF/2017/1.2.1.1 – “Environmental monitoring of wave and tidal devices”. This communication reflects only the author’s view. EASME is not responsible for any use that may be made of the information it contains.

